

ON THE ROTATION CLASS OF KNOTTED LEGENDRIAN TORI IN \mathbb{R}^5

SCOTT BALDRIDGE AND BEN MCCARTY

ABSTRACT. In this paper we show how to combinatorically compute the rotation class of a large family of embedded Legendrian tori in \mathbb{R}^5 with the standard contact form. In particular, we give a formula to compute the Maslov index for any loop on the torus and compute the Maslov number of the Legendrian torus. These formulas are a necessary component in computing contact homology. Our methods use a new way to represent knotted Legendrian tori called Lagrangian hypercube diagrams.

1. INTRODUCTION

Compared to Legendrian knots in \mathbb{R}^3 , little is known about knotted Legendrian submanifolds L^n embedded in \mathbb{R}^{2n+1} . One reason is that in higher dimensions there are no standard representations of embedded Legendrian submanifolds that enable one to study with the same facility as front projections or Lagrangian projections of Legendrian knots in \mathbb{R}^3 . For example, one may easily compute the classical invariants of Thurston-Bennequin and rotation numbers by looking at the front projection of a knot in \mathbb{R}^3 . Moreover, the classical invariants are quite effective at distinguishing many knots up to Legendrian isotopy: torus knots, for example have been shown to be classified by their classical invariants (cf. [10]).

While the Thurston-Bennequin number may be generalized to higher dimensions, it is not always as useful as it is for knots in dimension 3. In the case we study in this paper, knotted Legendrian tori $L \in \mathbb{R}^5$, the Thurston-Bennequin invariant is well defined (cf. [25]), but uninteresting since it is always equal to zero. In fact, the Thurston-Bennequin number in \mathbb{R}^{2n+1} equals $\frac{1}{2}\chi(L)$ when n is even. Furthermore, while topological knot type provides an additional invariant for Legendrian knots in \mathbb{R}^3 , all knotted Legendrian surfaces in \mathbb{R}^5 are topologically equivalent provided they are of the same genus.

The rotation class is harder to generalize to higher dimensions. Unlike the Thurston-Bennequin number, which may be defined in terms of a linking number, the rotation number requires the computation of the homotopy class of a map from L to the space of Lagrangians of \mathbb{R}^4 with symplectic structure induced by the contact form on \mathbb{R}^5 . Since writing down this map is non-trivial this invariant is more difficult to compute in higher dimensions.

Lagrangian hypercube diagrams overcome the difficulties involved in studying knotted Legendrian tori in \mathbb{R}^5 , by providing a way to construct explicit embeddings of Legendrian tori. Using the explicit map defined by a Lagrangian hypercube diagram we demonstrate that the rotation class may be calculated combinatorially as follows:

S. Baldridge was partially supported by NSF Grant DMS-0748636.

Theorem 1. *Given a Lagrangian hypercube diagram $H\Gamma = (C, \{\mathcal{W}, \mathcal{X}, \mathcal{Y}, \mathcal{Z}\}, G_{zx}, G_{wy})$ with Lagrangian grid diagram projections G_{zx} and G_{wy} in \mathbb{R}^2 , and let $L \subset \mathbb{R}^5$ be the embedded Legendrian torus determined by the lift of the Lagrangian torus defined by $H\Gamma$. Let $H_1(L) = \langle \tilde{\gamma}_{zx}, \tilde{\gamma}_{wy} \rangle$ be generated by $\tilde{\gamma}_{zx}$ and $\tilde{\gamma}_{wy}$ as in Theorem 6.1. Then, the rotation class of L , $r(L)$, satisfies:*

$$r(L) = (w(G_{zx}), w(G_{wy})),$$

where $w(G_{zx})$ is the winding number of the immersed curve determined by G_{zx} . In particular, the winding number can be computed combinatorially from the Lagrangian grid diagram projection:

$$w(G) = \frac{1}{4}(\#(\text{counterclockwise oriented corners of } G) - \#(\text{clockwise oriented corners of } G)).$$

Example 1.1. Let $H\Gamma$ be the Lagrangian hypercube diagram constructed from the Lagrangian grid diagrams shown in Figure 1 (Theorem 8.4). The Lagrangian hypercube determines an immersed Lagrangian torus T (Theorem 5.1). The lift of the Lagrangian torus T is a knotted, embedded Legendrian torus L (Theorem 6.1). By Theorem 1, the rotation class of the Legendrian torus L is $r(L) = (1, 0)$.

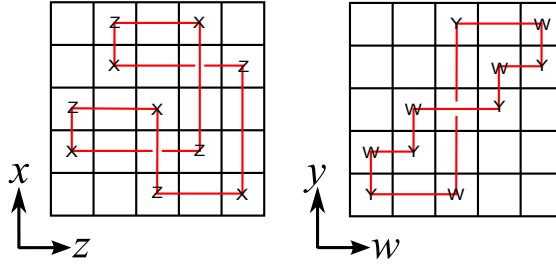


Figure 1: Unknots with rotation number 1 and 0 respectively..

Recall that the Maslov index, as defined in [23] and [9], may be viewed as a map $\mu : H_1(L) \rightarrow \mathbb{Z}$.

Corollary 2. *For $(a, b) \in H_1(L) = \langle \tilde{\gamma}_{zx}, \tilde{\gamma}_{wy} \rangle$, the Maslov index is*

$$\mu(A) = 2aw(G_{zx}) + 2bw(G_{wy}).$$

The Maslov number of the torus L is the smallest positive number that is the Maslov index of some nontrivial loop (cf. [9]). Thus Corollary 2 enables us to compute the Maslov number of L as follows:

Corollary 3. *The Maslov number of L is the non-negative number $2\gcd(w(G_{zx}), w(G_{wy}))$.*

In [9], Ekholm, Etnyre, and Sullivan compute the classical invariants for Legendrian tori obtained by front-spinning, showing that, in particular, the rotation class of the surface so obtained, is determined by the rotation number of the front projection used in the construction. Thus, their construction leads to tori with rotation class of the form $(0, r)$. Not only are we able to construct Legendrian tori in which both factors of the torus are knotted, but we show that Legendrian tori constructed from hypercube diagrams realize every possible pair of integers under the isomorphism defined by $H\Gamma$. In particular, we get examples where the rotation class is $(0, r)$ in the following theorem by taking one of the knots to be a trivial knot with rotation number zero:

Theorem 4. *Let $(m, k) \in \mathbb{Z}^2$, and K_1, K_2 be any two topological knots in \mathbb{R}^3 . Then there is a hypercube diagram, $H\Gamma = (C, \{\mathcal{W}, \mathcal{X}, \mathcal{Y}, \mathcal{Z}\}, G_{zx}, G_{wy})$ such that G_{zx} and G_{wy} are Lagrangian grid diagrams representing Legendrian knots in \mathbb{R}^3 with the same topological knot type as K_1 and K_2 . The Legendrian torus L determined by the lift of the Lagrangian torus determined by $H\Gamma$ satisfies $r(L) = (m, k)$.*

Theorem 4 is a statement about the existence of Lagrangian hypercube diagrams. The methods used in the proof to find Lagrangian hypercube diagrams lead in general to excessively large diagrams. In practice, however, Lagrangian hypercube diagrams are easy to build by hand. Knot theory benefited greatly because of the development of nice representations for the knots: braids, knot projections, grid diagrams, etc. Theorem 1 and 4 together can be viewed as our attempt to create similar useful representations of Legendrian tori in \mathbb{R}^5 . In fact, computers can be used to easily generate and compute examples (see Theorem 8.4).

This paper stands alone as one of the first papers to explicitly compute classical Legendrian invariants for a large class of knotted Legendrian submanifolds in \mathbb{R}^{2n+1} for $n \geq 2$ (cf. [9]). We see the potential for much more: this paper contains key elements in the computing the gradings and dimensions of the moduli spaces used in computing the differential in contact homology. Our future work will be on how to use the representations and the calculations in this paper to compute the contact homology algorithmically directly from Lagrangian hypercube diagrams.

In fact, we were particularly interested in studying the contact homology of embedded Legendrian tori in \mathbb{R}^5 (or S^5) because of their relationship to Special Lagrangian Cones used to study the String Theory Model in physics. Briefly, according to this model, our universe is a product of the standard Minkowsky space \mathbb{R}^4 with a Calabi-Yau 3-fold X . Based upon physical grounds, the SYZ-conjecture of Strominger, Yau, and Zaslov (cf. [24]) expects that this Calabi-Yau 3-fold can be given a fibration by Special Lagrangian 3-tori with possibly some singular fibers. To make this idea rigorous one needs control over the singularities, which are not understood well. One method used to study these singularities (cf. Haskins [12] and Joyce [13]) is to model them locally as special Lagrangian cones $C \subset \mathbb{C}^3$. A special Lagrangian cone can be characterized by its associated link $L = C \cap S^5$ (the link of the singularity), which turns out to be a minimal Legendrian surface. When the link type of L is a sphere, then C must be a special Lagrangian plane. The interesting tractable case appears to be when the link type is an embedded torus. Several authors (cf. Castro-Urbano [6], Haskins [12], Joyce [13]) have shown that there exist infinite families of nontrivial special Lagrangian cones arising from minimal embedded Legendrian tori. Some work is already being done by Aganagic, Ekholm, Ng, and Vafa [1] to understand the connection between contact homology and Lagrangian fillings. We see this paper as possibly laying groundwork for developing combinatorial tools to understand special Lagrangian cones through the lens of contact homology.

In Section 2 we present a definition for the rotation class in dimension 5 and prove that it is characterized by a pair of integers. Section 3 discusses Lagrangian grid diagrams, which enable us to define a Lagrangian hypercube diagram in Section 4. In Section 5 we prove that a Lagrangian hypercube diagram represents an immersed Lagrangian torus in dimension 4. This torus is shown in Section 6 to lift to a Legendrian torus in \mathbb{R}^5 with the standard contact structure. We then prove Theorem 1 (Section 7) and close with a proof of Theorem 4 and further examples (Section 8).

2. ROTATION CLASS FOR EMBEDDED LEGENDRIAN TORI IN \mathbb{R}^5

In [9] the classical Legendrian invariants of Thurston-Bennequin number and rotation number are generalized for \mathbb{R}^{2n+1} . We recall the definition of rotation class for \mathbb{R}^5 here. Let \mathbb{R}^5 be parametrized using $wxyz$ -coordinates. Then $\alpha = dt - ydw - xdz$ is a contact 1-form representing the standard contact structure on \mathbb{R}^5 . The contact hyperplanes are given by:

$$\xi = \ker(\alpha) = \{\partial_x, \partial_y, \partial_w + y\partial_t, \partial_z + x\partial_t\}.$$

Let $f : L \rightarrow (\mathbb{R}^5, \xi)$ be a Legendrian immersion. Then the image of $df_x : T_x L \rightarrow T_{f(x)}\mathbb{R}^5$ is a Lagrangian subspace of the contact hyperplane $\xi_{f(x)}$. Choose the complex structure $J : \xi_{(w,x,y,z,t)} \rightarrow \xi_{(w,x,y,z,t)}$ such that $J(\partial_w + y\partial_t) = \partial_y$, $J(\partial_y) = -(\partial_w + y\partial_t)$, $J(\partial_z + x\partial_t) = \partial_x$, and $J(\partial_x) = -(\partial_z + x\partial_t)$. Then the complexification $df_{\mathbb{C}} : TL \otimes \mathbb{C} \rightarrow \xi$ is a fiberwise bundle isomorphism. The homotopy class of $(f, df_{\mathbb{C}})$ is called the rotation class of L . Note that the Lagrangian projection $\pi_t : \mathbb{R}^5 \rightarrow \mathbb{C}^4$ gives a complex isomorphism between (ξ, J) and the trivial bundle with fiber \mathbb{C}^2 . Composing $df_{\mathbb{C}}$ with π_t we get a trivialization $TL \otimes \mathbb{C} \rightarrow \mathbb{C}^2$, which we identify with $df_{\mathbb{C}}$. Furthermore, we choose Hermitian metrics on $TL \otimes \mathbb{C}$ and \mathbb{C}^2 so that $df_{\mathbb{C}}$ is unitary. Thus f gives rise to an element of $U(TL \otimes \mathbb{C}, \mathbb{C}^2)$. The group of continuous maps $C(L, U(2))$ acts freely and transitively on $U(TL \otimes \mathbb{C}, \mathbb{C}^2)$ and hence $\pi_0(U(TL \otimes \mathbb{C}, \mathbb{C}^2))$ is in one to one correspondence with $[L, U(2)]$. From this point forward, we will consider $r(L)$ as an element $[L, U(2)]$.

In general, if L is a genus g Legendrian surface in \mathbb{R}^5 , then the rotation class is an element of $[\Sigma_g, U(2)]$. When $g = 0$, $[S^2, U(2)] \cong \pi_2(U(2))$, and hence, the rotation class is always trivial, and uninteresting (for spheres, neither classical invariant yields any useful information). However, when $g \geq 1$, the rotation class can be nontrivial. In fact,

Theorem 2.1. *The rotation class for a Legendrian torus can be thought of as an element in $\mathbb{Z} \times \mathbb{Z}$ via the isomorphism $[T, U(2)] \cong \pi_1(U(2)) \times \pi_1(U(2))$.*

Proof. Given a map of the standard torus, $i : T^2 \rightarrow \mathbb{R}^5$, let $a = i(1 \times S^1)$ and $b = i(S^1 \times 1)$. For $\pi_1(U(2))$, choose basepoint $1 \in U(2)$. Define $H : [T, U(2)] \rightarrow \pi_1(U(2)) \times \pi_1(U(2))$ to be the map $f \mapsto (f|_a, f|_b)$. H is surjective since $H(fg)(p, q) = (fg|_a(p), fg|_b(q)) = (f(p), g(q))$ for any pair $f, g \in \pi_1(U(2))$. The $\ker(H)$ is the set of homotopy classes of maps $f : T \rightarrow U(2)$ such that the $f|_{a \cup b}$ is nullhomotopic. Since $U(2)$ is aspherical, any map such that $f|_{a \cup b}$ is nullhomotopic must itself be nullhomotopic. Hence, the kernel is trivial and H is an isomorphism. \square

The existence of the isomorphism in Theorem 2.1 is, by itself, not useful in general for calculations due to the fact that the isomorphism depends heavily upon the choice of loops on the torus used to define the map: a generic embedding $i : T^2 \rightarrow \mathbb{R}^5$ does not have a preferred basis for homology (one can precompose with any element of $SL(2, \mathbb{Z})$ for example). However, Lagrangian hypercube diagrams do provide natural, albeit not canonical, choices for these loops as the torus is embedded in \mathbb{R}^5 (cf. $\tilde{\gamma}_{zx}$ and $\tilde{\gamma}_{wy}$ in Theorem 6.1). It is these choices together with Theorem 2.1 that allows us to write down our ‘‘preferred’’ calculations of rotation class and Maslov index for loops in the embedded Legendrian torus. The calculations are important to our future work in computing contact homology of knotted Legendrian tori algorithmically. While all of our calculations in computing the contact homology from a Lagrangian hypercube diagram will depend upon these choices, the contact homology calculation in the end will not.

Before moving on to the definition of a Lagrangian hypercube diagram, we begin with a discussion of Lagrangian grid diagrams.

3. LAGRANGIAN GRID DIAGRAMS

Let \mathbb{R}^3 be given wyt -coordinates. Then $\alpha = dt - ydw$ is a contact 1-form representing the standard contact structure on \mathbb{R}^3 . The contact planes are given by:

$$\xi = \ker(\alpha) = \{\partial_y, \partial_w + y\partial_t\}.$$

A Legendrian knot in (\mathbb{R}^3, ξ) is an embedding $L : S^1 \rightarrow \mathbb{R}^3$ whose tangent vectors always lie in the contact planes determined by ξ . Let $\theta \mapsto (w(\theta), y(\theta), t(\theta))$ be a parametrization of L . There are two standard projections used to study Legendrian knots, the front projection:

$$\Pi_L := \Pi \circ L : S^1 \rightarrow \mathbb{R}^2 : \theta \mapsto (w(\theta), t(\theta)),$$

and the Lagrangian projection:

$$\pi_L := \pi \circ L : S^1 \rightarrow \mathbb{R}^2 : \theta \mapsto (w(\theta), y(\theta)).$$

In general, a given knot diagram will not represent the Lagrangian projection of a Legendrian knot. However, an immersion $\gamma : S^1 \rightarrow \mathbb{R}^2 : \theta \mapsto (w(\theta), y(\theta))$ will correspond to the Lagrangian projection of a Legendrian knot in (\mathbb{R}^3, ξ) if the following hold:

$$(3.1) \quad \int_0^{2\pi} y(\theta)w'(\theta)d\theta = 0$$

$$(3.2) \quad \int_{\theta_0}^{\theta_1} y(\theta)w'(\theta)d\theta \neq 0 \text{ whenever } \theta_0 \neq \theta_1 \text{ and } \gamma(\theta_0) = \gamma(\theta_1).$$

We now translate 3.1 and 3.2 in the context of grid diagrams. Let \hat{G} be a wy -oriented grid diagram (cf. [2]). Grid diagrams have been studied extensively in [8], [14], [15], [20], [22], and consists of an $n \times n$ grid together with a set of markings that, when connected by edges, represent a knot diagram. Typically one assigns the y -parallel segments in \hat{G} to be the over-strands at any crossing. However, in the following definition we will ignore such crossing conditions, and think of \hat{G} as an immersed S^1 .

Definition 3.1. An *immersed grid diagram* is an oriented grid diagram G with no crossing data specified.

An immersed grid diagram G may be thought of as a mapping $\gamma : S^1 \rightarrow \mathbb{R}^2 : \theta \mapsto (w(\theta), y(\theta))$. Since $w'(\theta)$ is 0 along any segment in G parallel to the y -axis, and $y(\theta)$ is constant along any segment parallel to the w -axis, Condition 3.1 translates into

$$\int_0^{2\pi} y(\theta)w'(\theta)d\theta = \sum_{i=1}^n \sigma(a_i) \cdot y_i \cdot \text{length}(a_i) = 0,$$

where $\{a_i\}$ is the collection of segments of G parallel to the w -axis, y_i is the y -coordinate of a_i , and $\sigma(a_i)$ is +1 if a_i is oriented left to right and -1 otherwise. Given a crossing in G (i.e. given $\theta_0 < \theta_1$ such that $\gamma(\theta_0) = \gamma(\theta_1)$), Condition 3.2 becomes:

$$\int_{\theta_0}^{\theta_1} y(\theta)w'(\theta)d\theta = \sum_{i=1}^m \sigma(c_i) \cdot y_i \cdot \text{length}(c_i) \neq 0,$$

where $\{c_i\}$ is the set of w -parallel segments in the loop beginning and ending at the given crossing and such that $\gamma(\theta) \neq \gamma(\theta_0)$ for all $\theta \in (\theta_0, \theta_1)$. Condition 3.1 guarantees that choosing the other

loop $(\theta_1, \theta_0) \in \mathbb{R}/2\pi\mathbb{Z}$ will give the same integral up to sign as the one chosen. Therefore any immersed grid diagram G satisfying Conditions (1) and (2) lifts to a piecewise linear Legendrian knot in (\mathbb{R}^3, ξ) as follows: choose some $\theta_0 \in S^1$ and define the t -coordinate t_0 of $\gamma(\theta_0)$ to be 0. Then define

$$(3.3) \quad t_\theta = t_0 + \int_{\theta_0}^{\theta} y(u)w'(u)du.$$

Condition 3.1 guarantees that in defining the t -coordinate this way, the lift will be a closed loop. Condition 3.2 guarantees that the vertical and horizontal segments at a crossing will have different t -coordinates.

Definition 3.2. A *Lagrangian grid diagram* is an immersed grid diagram G satisfying Conditions 3.1 and 3.2.

Given a Lagrangian projection of a Legendrian knot L , one may compute the rotation number as follows. Use the vector field $w = \frac{\partial}{\partial y}$ to trivialize $\xi|_L$. Then the rotation number may be calculated to be the winding number of the tangent vector to L with respect to this trivialization:

$$r(L) = w(\pi_L).$$

For a Lagrangian grid, this is simply a signed count of the corners of G . Let B be the collection of corners in G . Then for a corner $b \in B$ let $\eta(b)$ be a function that assigns a value of $+1$ to any corner of type $W : NE$, $Y : NW$, $W : SW$, and $Y : SE$ (i.e. a counterclockwise oriented corner), and a value of -1 to any corner of type $W : NW$, $Y : NE$, $W : SE$, and $Y : SW$ (i.e. a clockwise oriented corner) following the same notation as in [22] and [21]. Figure 2 illustrates the types of corners. Thus we observe that:

Lemma 3.3. *Given a Lagrangian grid diagram G with Legendrian lift L , the rotation number satisfies:*

$$r(L) = w(G) = \frac{1}{4} \sum_{b \in B} \eta(b).$$

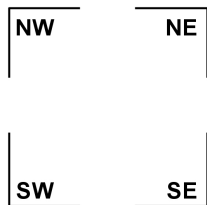


Figure 2: Types of corners in a grid diagram.

Example 3.4. Observe that $\int_G ydw = \frac{3}{2} + \frac{7}{2} - 2(\frac{5}{2}) = 0$, and for a path connecting the crossing to itself, $\int_G ydw = \frac{7}{2} - \frac{5}{2} = 1$. Hence, the unknot shown in Figure 3 is a Lagrangian grid. Set the t -coordinate of the w -mark in column 1 to 0 and define the lift as in Equation 3.3. Then the front projection corresponding to the lift of G is shown in Figure 3. The rotation number is easily computed from this projection since G has 3 bends that are assigned a value of $+1$ and 3 that are assigned a value of -1 . Hence, $r(G) = 0$.

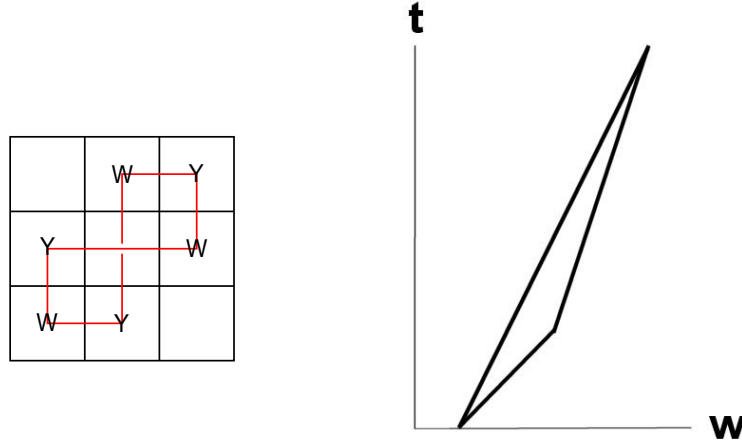


Figure 3: A wy immersed grid diagram for the unknot and its corresponding front projection.

The Legendrian knots produced using the above method will be piecewise linear, not smooth. However, we can produce smoothly embedded knots as follows. Choose $0 < \epsilon \ll 1$. Delete an ϵ neighborhood of each vertex of G and replace it with a smooth curve (cf. Figure 4). Such a smoothing may be accomplished so as to guarantee that the diagram is smooth at the boundary of the ϵ neighborhood as well. For example, the image of the map

$$E(t) = (w + \epsilon - \epsilon \cos(t/\epsilon), y + \epsilon - \epsilon \sin(t/\epsilon)).$$

allows one to replace a $W : SE$ corner with a smooth arc, but the resulting rounded corner will only be C^1 at the boundary of the ϵ neighborhood. Note that the smoothing may be done so that the resulting curve is symmetric about the line of slope ± 1 through the vertex of the bend. Furthermore, given a choice of a smoothing at a corner such that the area enclosed by the smooth curve and the original bend is A , one may obtain a different smoothing so that the area enclosed is rA where $r \in \mathbb{R}$ such that $0 < r \leq 1$.

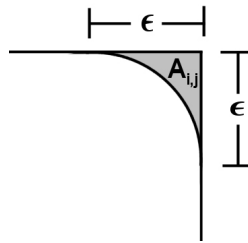


Figure 4: A smoothing of a corner.

Proposition 3.5. *Let $\gamma : S^1 \rightarrow \mathbb{R}^2$ be the piecewise linear immersion determined by the Lagrangian grid diagram, G . There exists a $\delta > 0$ such that for any $0 < \epsilon \leq \delta$ there is a choice of smoothing curves based upon ϵ such that the immersion determined by the smoothed grid, $\gamma_\epsilon : S^1 \rightarrow \mathbb{R}^2$ satisfies the following:*

- the lift of γ_ϵ is C^0 -close to the lift of γ , and
- for any two $\epsilon, \epsilon' < \delta$ the Legendrian knots K, K' are Legendrian isotopic.

Proof. Choose $\delta > 0$ such that $\delta^2 < \frac{1}{2n}$. Let $\epsilon < \delta/2$. Enumerate the corners $b_{i,j} \in B$ so that corner $b_{i,1}$ is the corner on the lefthand side of row i and $b_{i,2}$ is the corner on the righthand side of row i . Let $A_{i,j}$ be the absolute value of the area of the region enclosed by the smoothed arc and the original corner of the corner $b_{i,j} \in B$. Construct each smoothing so that $|A_{i,j}| \leq \epsilon$. Denote by r_i the horizontal edge in row i . Then we have the following:

$$\int_G ydw = \sum_{i=1}^n \sigma(r_i) \cdot (i \cdot \text{length}(r_i) - \tau_1(i)A_{i,1} - \tau_2(i)A_{i,2}) = - \sum_{i=1}^n \sigma(r_i) \cdot (\tau_1(i)A_{i,1} + \tau_2(i)A_{i,2})$$

where $\sigma(r_i)$ is $+1$ if the edge is directed left to right and -1 otherwise, $\tau_j(i)$ is $+1$ if the smoothing lies above the horizontal edge, and -1 otherwise.

Since not all of $\sigma(r_i) \cdot \tau_1(i)$ will evaluate to $+1$ (respectively, all -1), we may choose the smoothings so that

$$\sum_{i=1}^n \sigma(r_i) \cdot (\tau_1(i)A_{i,1} + \tau_2(i)A_{i,2}) = 0.$$

Since the value of the integral in Equation 3.2 may only change from the piecewise linear calculation by an amount less than $\frac{1}{4}$, the smoothed diagram has the same crossing data as the original Lagrangian grid diagram. The second condition of the Lemma is clear. \square

Note if $A_{i,j} = A$ for all i, j , the above sum evaluates to $4Ar(G)$. Thus, if the rotation number is 0 then the same smoothing may be used for all vertices of G .

Corollary 3.6. *Let γ_ϵ be parametrized by $\theta \mapsto (w(\theta), y(\theta))$. Then,*

$$\left| \int_{\theta_0}^{\theta_1} y(\theta)w'(\theta)d\theta - \int_{\theta_0}^{\theta_1} y_\epsilon(\theta)w'_\epsilon(\theta)d\theta \right| < \frac{1}{4}.$$

Proposition 3.5 and Corollary 3.6 show that a Lagrangian grid diagram corresponds to a smoothly embedded Legendrian knot that does not depend on the choice of epsilon used in the smoothing. Hence we may refer to *the Legendrian knot* corresponding to a Lagrangian grid diagram.

Example 3.7. Since the rotation number of the unknot in Figure 3 is 0 we may choose to smooth all corners in the same way, thus obtaining a Lagrangian projection of a smoothly embedded Legendrian knot in (\mathbb{R}^3, ξ) .

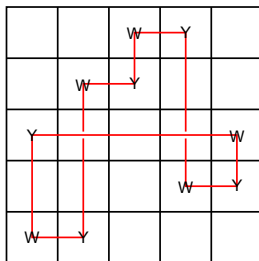


Figure 5: An unknot with rotation number 1.

Example 3.8. The unknot shown in Figure 5 may easily be seen to have rotation number 1. In order to smooth the diagram, we perform the following calculation. To simplify matters choose the smoothings so that the areas satisfy $A_{i,1} = A_{i,2}$, $A_i = A_{i,j}$, and all are less than $\frac{1}{100}$.

$$\sum_{i=1}^n \sigma(r_i) \cdot (\tau_1(i)A_i + \tau_2(i)A_i) = 2A_1 + 2A_2 + 2A_3 - A_4 + A_4 - 2A_5$$

Choose the A_i so that $A_1 = A_2 = A_3$ and $A_5 = 3A_1$. Then this sum will be 0 and the Lagrangian grid conditions will still be satisfied by the smoothed diagram, and the diagram will be the Lagrangian projection of a smoothly embedded Legendrian knot in (\mathbb{R}^3, ξ) .

The Legendrian lift of the smoothed Lagrangian grid diagram is unique up to Legendrian isotopy (Proposition 3.5). By Corollary 3.6 we can do integer calculations directly from the Lagrangian grid diagram instead of the smooth γ_ϵ loop, without worrying about changing the crossing information of the lift of the Lagrangian grid diagram. In particular, there is a correspondence of horizontal edges with opposite orientation in each column that allows one to re-interpret the Lagrangian grid conditions as a signed area sum. That is:

Corollary 3.9. *There is a set of rectangles (possibly overlapping) with horizontal edges lying on the knot diagram whose signed areas sum to the same value as the integral in Equation 3.3.*

Example 3.10. For the grid diagram in Figure 6, we see by computing the signed areas shown that the integral in Equation 3.3 evaluate to -7 . Hence, it is not a Lagrangian grid diagram.

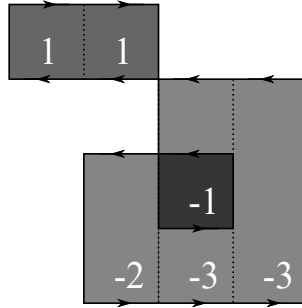


Figure 6: Decomposition of grid into rectangles.

In practice, the area calculation described in the previous example may be carried out by simply decomposing the grid into polygonal regions where the top-most horizontal edges are all oriented left (resp. right) and the bottom-most horizontal edges are all oriented right (resp. left). Then, the signed area of these polygonal regions will correspond to the integrals defined in Conditions 3.1 and 3.2. For convenience, in the proofs that follow, we will use this signed area calculation to compute the integrals defined in Conditions 3.1 and 3.2.

Theorem 3.11. *Any topological knot type with any rotation number may be realized as a Lagrangian grid diagram.*

Before proving the theorem, we introduce some definitions and lemmas that we will use only for the proofs in this paper.

Definition 3.12. An *almost Lagrangian grid diagram* is an immersed grid diagram such that:

- the top right corner has a marking,

- there is a parametrization $\gamma : I \rightarrow G \subset \mathbb{R}^2$ in which $\gamma(\theta)$ starts and ends at that marking point.
- $\int_{\theta_1}^{\theta_2} y(\theta)w'(\theta)d\theta \neq 0$ whenever $\theta_1, \theta_2 \in (0, 1)$, $\theta_1 \neq \theta_2$ and $\gamma(\theta_1) = \gamma(\theta_2)$.

Let the t -coordinate of $\gamma(0)$ be 0. Then define,

$$t_\theta = \int_0^\theta y(u)w'(u)du.$$

Thus the last condition of Definition 3.12 guarantees that an almost Lagrangian grid diagram gives rise to an embedded Legendrian arc. Since the endpoints of this arc project to the top right corner marking and differ only in their t -coordinates, an almost Lagrangian grid diagram still gives rise to a knot in \mathbb{R}^3 by attaching the endpoints by a segment parallel to the t -axis.

Lemma 3.13. *An almost Lagrangian grid diagram can always be modified (using configurations listed in Table 1) to get a Lagrangian grid diagram with the same topological knot type and winding number as the knot given by the almost Lagrangian grid diagram.*

Proof. An almost Lagrangian grid diagram represents a Legendrian arc whose endpoints have t -coordinates that differ by some $k \in \mathbb{Z}$. Attach one of the configurations shown in Table 1. Each time such a configuration is attached, the resulting grid will again be an almost Lagrangian grid diagram, but the difference between the end points of the new Legendrian arc will be reduced by 1 or 2. Continue reducing this difference until the arc closes up to give a Lagrangian grid diagram. \square

$\Delta t:$	-2	-1	1	2

TABLE 1. Configurations used to convert an almost Lagrangian grid diagram into a Lagrangian grid diagram. The value of Δt follows from Corollary 3.9.

Lemma 3.14. *Let $k \in \mathbb{Z}$. Any Lagrangian grid diagram can be modified to obtain a Lagrangian grid diagram with rotation number k .*

Proof. Let $k \in \mathbb{Z}$. If the Lagrangian grid diagram does not have a marking in the top right corner, modify it so that does by stabilizing in the righthand column and commuting the horizontal edge of length 1 to the top of the grid, to obtain an almost Lagrangian grid diagram. Then, at this top right corner, attach one of the configurations shown in Figure 7 to change the rotation number to k . This new object is an almost Lagrangian grid diagram. Apply Lemma 3.13 to obtain a Lagrangian grid diagram whose lift has the same topological knot type as the original Lagrangian grid diagram. \square

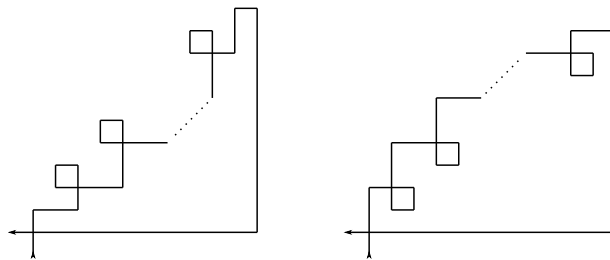


Figure 7: Configuration to change the winding number of an immersed grid diagram.

We now proceed with the proof of Theorem 3.11.

Proof. We use Lenhard Ng's arguments, [19], as a guide to construct Lagrangian grid diagrams. Recall that a grid diagram (in the usual sense) may be thought of as a front projection of a Legendrian knot. Given such a front projection, we may resolve the front to obtain the Lagrangian projection of a knot isotopic to the one determined by the front. This Lagrangian projection will have the same crossing data as the original grid, and, as a diagram, is isotopic to the original grid after adding loops at each southeast corner.

We follow a similar procedure, but modify it so that we obtain a Lagrangian grid diagram. Given a grid diagram (in the usual sense), stabilize at each southeast corner (without adding a crossing), and commute the horizontal edge of length 1 to the bottom of the grid to obtain a simple front (cf. [19]). By applying another stabilization in the right-most column, and then commutation moves, we may ensure that this grid has a marking in the top right corner. Then add a loop at each southeast corner, as is done in constructing the front resolution. By possibly inserting some number of empty rows and columns, we may adjust the enclosed areas so that we obtain a diagram whose lift represents the same knot in \mathbb{R}^3 as the grid diagram we started with. This diagram will, in general, not be a grid diagram, since it contains empty rows and columns. At the top right corner, attach a configuration as shown in Figure 8 to fill in any empty rows and columns, and thus obtain an almost Lagrangian grid diagram. Then, by applying Lemmas 3.13 and 3.14, we may obtain a Lagrangian grid diagram representing the same topological knot type as the original grid diagram, and having any rotation number k . \square

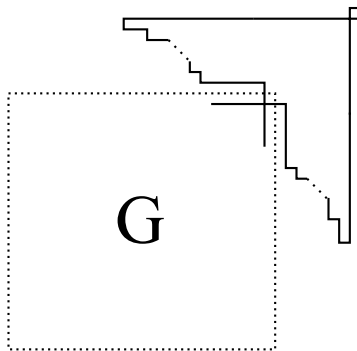


Figure 8: Filling in empty rows and columns.

4. LAGRANGIAN HYPERCUBE DIAGRAMS IN DIMENSION 4

The definition of a Lagrangian hypercube diagram codifies a data structure that mimics that of hypercube diagrams, cube diagrams and grid diagrams. While the definition appears similar to that of 4-dimensional hypercube diagrams as defined in [2], they are not equivalent. Let n be a positive integer and let the hypercube $C = [0, n] \times [0, n] \times [0, n] \times [0, n] \subset \mathbb{R}^4$ be thought of as a 4-dimensional Cartesian grid, i.e., a grid with integer valued vertices with axes w , x , y , and z . Orient \mathbb{R}^4 with the orientation $w \wedge x \wedge y \wedge z$.

A *flat* is any right rectangular 4-dimensional prism with integer valued vertices in the hypercube such that there are two orthogonal edges at a vertex of length n and the remaining two orthogonal edges are of length 1. Name flats by the axes parallel to the two orthogonal edges of length n . For example, a yz -flat is a flat that has a face that is an $n \times n$ square that is parallel to the yz -plane.

Similarly, a *cube* is any right rectangular 4-dimensional prism with integer vertices in the hypercube such that there are three orthogonal edges of length n at a vertex with the remaining orthogonal edge of length 1. Name cubes by the three edges of the cube of length n . See Figure 9 for examples.

A marking is a labeled point in \mathbb{R}^4 with half-integer coordinates. Mark unit hypercubes in the 4-dimensional Cartesian grid with either a W , X , Y , or Z such that the following *marking conditions* hold:

- each cube has exactly one W , one X , one Y , and one Z marking;
- each cube has exactly two flats containing exactly 3 markings in each;
- for each flat containing exactly 3 markings, the markings in that flat form a right angle such that each ray is parallel to a coordinate axis;
- for each flat containing exactly 3 markings, the marking that is the vertex of the right angle is W if and only if the flat is a zw -flat, X if and only if the flat is a wx -flat, Y if and only if the flat is a xy -flat, and Z if and only if the flat is a yz -flat.

The 4th condition rules out the possibility of either wy -flats or a zx -flats with three markings. As with oriented grid diagrams and cube diagrams, we obtain an oriented link from the markings by connecting each W marking to an X marking by a segment parallel to the w -axis, each X marking to a W marking by a segment parallel to the x -axis, and so on.

Let $\pi_{xz}, \pi_{wy} : \mathbb{R}^4 \rightarrow \mathbb{R}^2$ be the natural projections. Define $G_{wy} := \pi_{xz}(C)$ and $G_{zx} := \pi_{wy}(C)$ which are immersed grid diagrams. Let $\{c_i\}$ be the crossings in G_{zx} , and $\{c'_i\}$ be the crossings in G_{wy} . Then we say that the *Lagrangian crossing conditions* hold for the pair G_{zx} and G_{wy} if $|\Delta t(c_i)| \neq |\Delta t(c'_i)| \forall i, j$ where Δt is the difference in the t -coordinates at each crossing determined by Equation 3.2.

Definition 4.1. If the markings $\{W, X, Y, Z\}$ in C satisfy the marking conditions, and the immersed grid diagrams G_{wy} and G_{zx} are Lagrangian grid diagrams satisfying the Lagrangian crossing conditions, then we define $H\Gamma = (C, \{W, X, Y, Z\}, G_{zx}, G_{wy})$ to be a *Lagrangian hypercube diagram*.

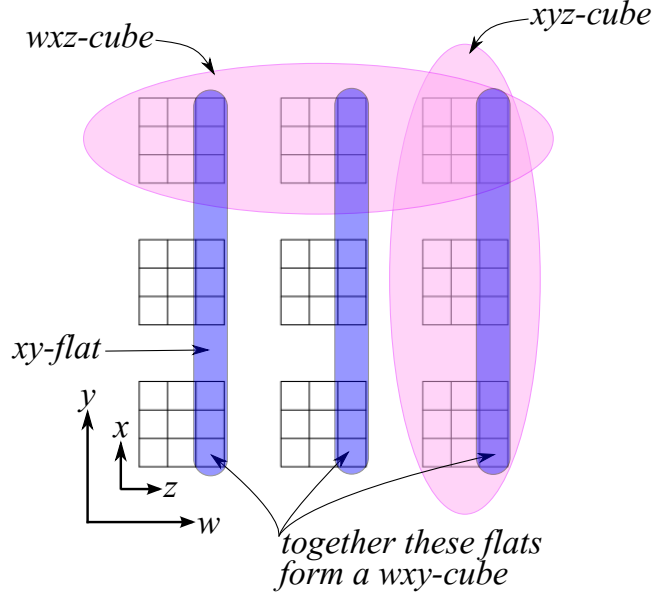


Figure 9: A schematic for displaying a Lagrangian hypercube diagram. The outer w and y coordinates indicate the “level” of each zx -flat. The inner z and x coordinates start at $(0, 0)$ for each of the nine yz -flats. With these conventions understood, it is then easy to display xy -flats, xyz -cubes, wxz -cubes, wxy -cubes, etc.

5. BUILDING A TORUS FROM A LAGRANGIAN HYPERCUBE DIAGRAM

A hypercube schematic (cf. Figure 10) conveniently displays the markings of a Lagrangian hypercube diagram so that the Lagrangian grid diagrams G_{zx} and G_{wy} may be read off of the diagrams directly. To see G_{wy} treat each $n \times n$ zx -flat as a cell of G_{wy} (i.e. consider the projection $\pi_x \circ \pi_z$). Each zx -flat containing a W and Z marking will project to a cell of G_{wy} containing a W marking and each zx -flat containing an X and Y marking will project to a cell of G_{wy} containing a Y marking. In Figure 10, the blue shading indicates the diagram associated to G_{wy} . To see G_{zx} in the schematic, note that each pair of markings in a zx -flat on the schematic corresponds to an edge of the Lagrangian grid diagram G_{zx} . Placing these segments on a single $n \times n$ grid will produce a copy of G_{zx} .

To produce an immersed torus from the Lagrangian hypercube diagram, place a copy of the immersed grid G_{zx} at each zx -flat on the schematic that contains a pair of markings (shown in red on Figure 10). Doing so produces a schematic with two copies of G_{zx} with the same y -coordinates and two with the same w -coordinates. For each pair of copies sharing the same w -coordinates, we may translate one parallel to the w -axis toward the other. Doing so traces out an immersed tube connecting these two copies of G_{zx} . Similarly, we may translate parallel to the y -axis to produce an immersed tube connecting two copies of G_{zx} with the same y -coordinates. Since we are connecting copies of G_{zx} in flats corresponding to the markings of G_{wy} , the tube will close to produce an immersed torus. Thus we obtain:

Theorem 5.1. *A Lagrangian hypercube diagram determines an immersed Lagrangian torus $i : T \rightarrow \mathbb{R}^4$. Furthermore, the map determines a preferred set of loops, $\gamma_{zx} = S^1 \times 1$ and $\gamma_{wy} = 1 \times S^1$, that map to curves projecting to the Lagrangian grid diagrams G_{zx} and G_{wy} .*

Since the torus is formed by the translation of x and z -parallel segments to the w and y axes, we see that only wx , wz , yz , and xy rectangles are used in the construction of the torus. Since wy and zx rectangles are never used in the construction of the torus, it is Lagrangian with respect to the symplectic form $dw \wedge dy + dz \wedge dx$. Furthermore, just as in the case of Lagrangian grid diagrams, we obtained a smooth embedding by carefully smoothing corners, we may obtain a smooth embedding of the torus in \mathbb{R}^5 by first smoothing G_{zx} and G_{wy} as in Lemma 3.5.

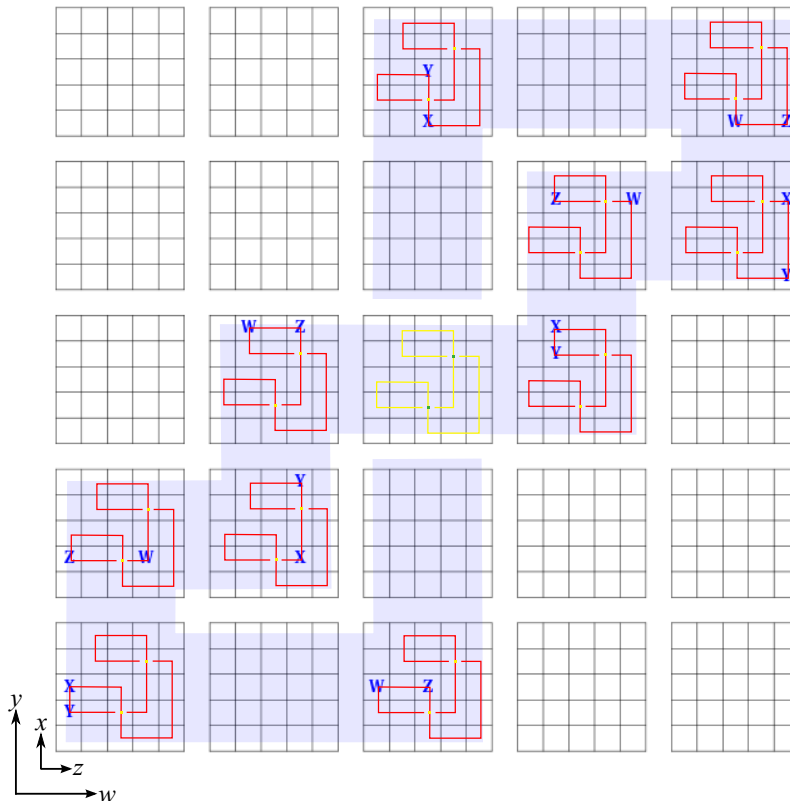


Figure 10: Lagrangian hypercube diagram with unknotted G_{zx} and G_{wy} and rotation class $(1, 0)$.

Furthermore, the torus has only two types of singularities: double point circles and intersections of double point circles. Each crossing of G_{zx} generates a double point circle as shown by the yellow dots in Figure 10. Similarly each crossing of G_{wy} generates a double point circle, which is visible in the schematic as the zx -flat where a w -parallel tube passes through a y -parallel tube. In Figure 10 this is shown by the yellow diagram. The green dot in Figure 10 corresponds to an intersection of two double point circles.

6. LIFTING THE HYPERCUBE TO \mathbb{R}^5

Let $i : T \rightarrow \mathbb{R}^4$ be the immersed torus obtained from a Lagrangian hypercube diagram as given by Theorem 5.1. Note that, $d\alpha|_{wxyz\text{-hyperplane}} = \omega = dw \wedge dy + dz \wedge dx$ is a symplectic form on \mathbb{R}^5 . We will show that HT represents the Lagrangian projection of a Legendrian surface in \mathbb{R}^5 with respect to the standard contact structure ξ .

In order to lift $i(T)$ we begin by choosing some point $p \in i(T)$ to have t coordinate equal to some $t_0 \in \mathbb{R}$. If we attempt to lift $i(T)$ to a Legendrian surface with respect to α we should choose to define the t -coordinate of $p' \neq p$ to be:

$$(6.1) \quad t = t_0 + \int_{\gamma} ydw + \int_{\gamma} xdz,$$

where γ is a path from p to p' . This integral will be independent of path precisely when the 1-form $i^*(ydw + xdz)$ is 0 on $H_1(T)$. Recall that $H_1(T)$ is generated by γ_{zx} and γ_{wy} .

In order check for path-independence of the integral in Equation 6.1, we evaluate the following:

$$(6.2) \quad i^*(ydw + xdz)[i^*(\gamma_{zx})] = \int_{i^*(\gamma_{zx})} i^*(ydw + xdz) = \int_{\gamma_{zx}} ydw + \int_{\gamma_{zx}} xdz = \int_{\gamma_{zx}} ydw.$$

$$(6.3) \quad i^*(ydw + xdz)[i^*(\gamma_{wy})] = \int_{i^*(\gamma_{wy})} i^*(ydw + xdz) = \int_{\gamma_{wy}} ydw + \int_{\gamma_{wy}} xdz = \int_{\gamma_{wy}} xdz.$$

Since G_{zx} and G_{wy} are Lagrangian grid diagrams, these integrals will both evaluate to 0 and we get a well-defined lift to a Legendrian torus in \mathbb{R}^5 using Equation 6.1. Furthermore, the Lagrangian crossing conditions guarantee that the lift will be embedded. Let L be the lift of $i(T)$ obtained from Equation 6.1. Define $\pi_t : \mathbb{R}^5 \rightarrow \mathbb{R}^4$ to be the projection $(w, x, y, z, t) \mapsto (w, x, y, z)$. Then $\pi_t(L) = i(T)$, i.e. the torus determined by $H\Gamma$ is the Lagrangian projection of the Legendrian torus L . Thus we obtain the following:

Theorem 6.1. *The torus determined by a Lagrangian hypercube diagram $H\Gamma$ lifts to an embedded Legendrian torus $L \subset (\mathbb{R}^5, \xi)$. Furthermore, the generators γ_{zx} and γ_{wy} lift to curves $\tilde{\gamma}_{zx}$ and $\tilde{\gamma}_{wy}$ that generate $H_1(L)$.*

Remark 6.2. If we omit the Lagrangian crossing conditions from the definition of a Lagrangian hypercube diagram, then the above procedure will still produce an *immersed* Legendrian torus in \mathbb{R}^5 , but it will not, in general, be embedded.

Example 6.3. Figure 10 shows a schematic picture of a Lagrangian hypercube diagram where all grid-projections are unknots as in Example 3.4. By Lemma 6.1, the torus determined by this Lagrangian hypercube diagram lifts to a Legendrian torus in (\mathbb{R}^5, ξ) .

7. PROOF OF THEOREM 1

With the rotation class understood to be an element of $[T, U(2)]$ we see from Theorem 2.1 that the class may be identified with a pair of integers corresponding to the elements of $\pi_1(U(2))$ determined by a meridian and longitude of the torus. Before proving Theorem 1 we identify an explicit generator of $\pi_1(U(2))$. Recall that $U(2)$ parametrizes *framed* Lagrangians of (\mathbb{R}^2, ω) . Identify the yx , xy , yz , and zy planes with the following matrices:

$$U_{xy} = \begin{pmatrix} 0 & i \\ i & 0 \end{pmatrix}, U_{yx} = \begin{pmatrix} 0 & i \\ -i & 0 \end{pmatrix}, U_{yz} = \begin{pmatrix} 0 & i \\ -1 & 0 \end{pmatrix}, U_{zy} = \begin{pmatrix} 0 & i \\ 1 & 0 \end{pmatrix}.$$

Note that U_{xy} , U_{yx} , U_{yz} , and U_{zy} correspond to unitary Lagrangian frames (cf. [18]):

$$U_{xy} \mapsto \begin{pmatrix} 0 & 0 \\ 0 & 0 \\ 0 & 1 \\ 1 & 0 \end{pmatrix}, U_{yx} \mapsto \begin{pmatrix} 0 & 0 \\ 0 & 0 \\ 0 & 1 \\ -1 & 0 \end{pmatrix}, U_{yz} \mapsto \begin{pmatrix} 0 & 0 \\ -1 & 0 \\ 0 & 1 \\ 0 & 0 \end{pmatrix}, U_{zy} \mapsto \begin{pmatrix} 0 & 0 \\ 1 & 0 \\ 0 & 1 \\ 0 & 0 \end{pmatrix},$$

Note that as maps from $\mathbb{R}^2 \rightarrow \mathbb{R}^4$ these frames produce xy , $(-x)y$, $(-z)y$, and zy -planes respectively. Geometrically, this matches up with the fact that the Lagrangian planes along an xz -slice of the hypercube will be given by a positively or negatively oriented ∂_x or ∂_z vector paired with a positively oriented ∂_y -vector.

Choose U_{xy} to be the basepoint. We define a loop $\gamma : [0, 1] \rightarrow U(2)$ that begins at U_{xy} and rotates through U_{yz} , U_{yx} and U_{zy} . We will define γ in 4 pieces. First, define a map $\hat{\gamma} : [0, 1] \rightarrow U(2)$ as follows:

$$\hat{\gamma}(t) = \begin{pmatrix} 1 & 0 \\ 0 & e^{\frac{\pi}{2}it} \end{pmatrix}.$$

Then, define $\gamma_1(t) = \hat{\gamma}(t)U_{xy}$, $\gamma_2(t) = \hat{\gamma}(t)U_{yz}$, $\gamma_3(t) = \hat{\gamma}(t)U_{yx}$, and $\gamma_4(t) = \hat{\gamma}(t)U_{zy}$. Finally, define $\gamma(t) = \gamma_1 \star \gamma_2 \star \gamma_3 \star \gamma_4$. Thus γ corresponds to a rotation of Lagrangian planes, beginning at an xy -plane, and rotating through yz , yx , and zy -planes.

Lemma 7.1. *The loop γ represents a generator of $\pi_1(U(2))$.*

Proof. Observe that the determinant, $\det : U(2) \rightarrow U(1)$ induces an isomorphism on π_1 that takes γ to a generator of $\pi_1(U(1))$. \square

The same argument will show that there is a generator for $\pi_1(U(2))$ given by acting on matrices U_{xy} , \hat{U}_{yx} , U_{xw} , and U_{wx} on the left by:

$$\tilde{\gamma}(t) = \begin{pmatrix} e^{\frac{\pi}{2}it} & 0 \\ 0 & 1 \end{pmatrix}.$$

Note that $U_{yx} \neq \hat{U}_{yx}$ as matrices in $U(2)$ but they give rise to the same Lagrangian planes, with the same orientation. While U_{yx} corresponds to a unitary Lagrangian frame giving rise to the Lagrangian plane $\{-\partial_x, \partial_y\}$, \hat{U}_{yx} gives rise to the Lagrangian plane $\{\partial_x, -\partial_y\}$.

Much of the content of the paper to this point has been building up toward presenting the following proof. Our discussion of Lagrangian grid diagrams in Section 3 enables us to define an immersed Lagrangian torus corresponding to a Lagrangian hypercube diagram as in Theorem 5.1. Lemma 6.1 shows how to obtain a Legendrian torus from the Lagrangian hypercube diagram. Having determined easy methods for computing the rotation number of the Lagrangian grid diagrams (Lemma 3.3), we are ready to prove Theorem 1.

Proof. Lemma 6.1 guarantees that the lift, L , exists. We must see that the image of $r(L) \in [T, U(2)]$ under the isomorphism defined in Theorem 2.1 is $(w(G_{zx}), w(G_{wy}))$. G_{zx} and G_{wy} each correspond to one of the two factors of T . Let $[f_{zx}]$ and $[f_{wy}]$ be the elements of $\pi_1(U(2))$ determined by G_{zx} and G_{wy} (since G_{zx} and G_{wy} are constant, choice of base point is irrelevant). Then the isomorphism defined in Theorem 2.1 maps $r(L)$ to $([f_{zx}], [f_{wy}])$. We must show that $[f_{zx}] = w(G_{zx})[\gamma]$.

Clearly, $w(G_{zx})$ computes how many times the tangent vector to the grid G_{zx} wraps around the loop γ . By Lemma 7.1 $[\gamma]$ generates $\pi_1(U(2))$. A similar argument shows that $[f_{wy}] = w(G_{wy})[\gamma]$. \square

Corollary 2 *Let $H_1(T_{H\Gamma})$ be generated by $i(\gamma_1)$ and $i(\gamma_2)$ (as in Theorem 5.1). The Maslov index, $\mu : H_1(T_{H\Gamma}) \rightarrow \mathbb{Z}$ can be computed directly. For $A = (a, b) \in H_1(T_{H\Gamma})$,*

$$\mu(A) = 2aw(G_{zx}) + 2bw(G_{wy})$$

Proof. Given an embedded loop $\gamma : S^1 \rightarrow T_{H\Gamma}$ representing a primitive class $A \in H_1(T_{H\Gamma})$, for any $p \in S^1$, $T_{\gamma(p)}T_{H\Gamma}$ is a Lagrangian plane, $L_{\gamma(p)}$. Thus we obtain a map $S^1 \rightarrow \text{Lag}(\mathbb{C}^2)$ such that $p \mapsto L_{\gamma(p)}$. The isomorphism defined in the proof of Theorem 1 is valid here as well, once we identify planes that differ only in orientation, which produces a factor of 2. \square

Corollary 3 *The Maslov number is $2\gcd(w(G_{zx}), w(G_{wy}))$.*

Proof. Follows directly from the previous corollary and the fact that the Maslov number is the smallest positive number that is the Maslov index of a non-trivial loop in $H_1(T_{H\Gamma})$ and 0 if every non-trivial loop has Maslov index 0 (cf. [9]). \square

8. PROOF OF THEOREM 4 AND EXAMPLES

Before proceeding with the proof of Theorem 4 we establish a few preliminary results. The construction of Theorem 8.4 can be used to produce a hypercube diagram (in the sense of [2]) given any pair of Lagrangian grid diagrams. However if the Lagrangian crossing conditions are not satisfied by the pair of Lagrangian grid diagrams, the resulting Legendrian torus will not be embedded (cf. Remark 6.2). Theorem 8.1, 8.2, and Corollary 8.3 show that for any pair of topological knots, and any rotation numbers, one may find a pair of Lagrangian grid diagrams such that the Lagrangian crossing conditions are satisfied and hence construct a Lagrangian hypercube diagram that lifts to an embedded Legendrian torus.

Theorem 8.1. *Let G be a Lagrangian grid diagram with an upper-right corner. Enumerate the crossings of G by $\{c_i\}$. Then, for any $M > 0$ there is another Lagrangian grid diagram G' , representing the same topological knot and having the same rotation number as G , such that $|\Delta t(c'_i)| > M$ for all i .*

Proof. Scale G by $k \in \mathbb{Z}$ (each segment of the diagram of length ℓ becomes a segment of length $k\ell$). This produces a diagram satisfying the Lagrangian conditions (Equations 3.1 and 3.2), but, of course, it will not be a grid diagram, due to empty rows and columns. However, the area of each rectangle (as in Corollary 3.9) will be multiplied by k^2 . Therefore, $|\Delta t(c_i)|$ may be made arbitrarily large for all i . We must then show that the empty rows and columns may be filled in, while preserving the Lagrangian grid conditions.

By following the techniques of Theorem 3.11 we may assume that the upper-right corner of G (prior to scaling) has a horizontal and vertical edge of length 1 or 2. Begin by inserting one additional row and column at the upper-right corner. The additional area created by this will be either $2k + 1$, $3k + 1$, or $4k + 1$ depending on the initial lengths of the horizontal and vertical edges of the upper-right corner. Then attach the configuration shown in Figure 11. The unshaded regions will be equal in area, but with opposite sign due to the symmetry between empty rows and columns after scaling the initial grid. The dark-grey regions will also be equal in magnitude but with opposite sign. Finally the light-grey region at the top right may be extended so that it is of area $2k + 1$, $3k + 1$, or $4k + 1$ (an even or odd area may be achieved by placing an additional box as shown by the dotted lines at the upper-right corner of Figure 11).

Finally, observe that for all of the original crossings, Δt has been scaled up by a factor of k^2 . However, this procedure creates 4 additional crossings: d_1 , d_2 , d_3 , and d_4 . By choosing k sufficiently large, and possibly making our initial grid diagram larger, we may ensure that $\min|\Delta t(d_i)| \geq jk + 1$ for $j = 2, 3, 4$. \square

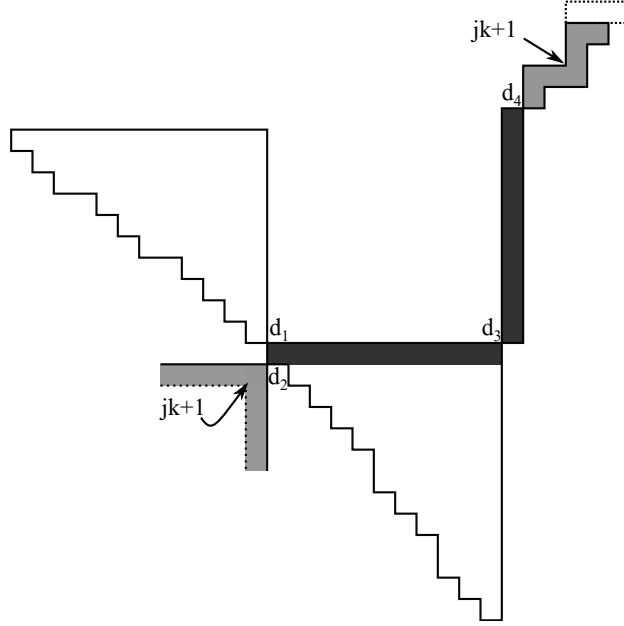


Figure 11: Configurations used to fill in empty rows and columns ($j = 2, 3, 4$).

We showed in the previous theorem that the minimum value of $|\Delta t(C_i)|$ may be made arbitrarily large for a Lagrangian grid diagram, the following theorem shows that we may make Lagrangian grid diagrams arbitrarily large, while keeping $\Delta t(c_i)$ small.

Theorem 8.2. *Given a Lagrangian grid diagram G of size n , there exists $m > n$ such that one may modify G to obtain a Lagrangian grid diagram, G' of size n' for any $n' > m$, with the same topological type and rotation number as G . Moreover, if Δ_1 is the maximum over $|\Delta t(c_i)|$ for G and Δ_2 is defined similarly for G' , then $\Delta_2 \leq \Delta_1 + |a| + 1$.*

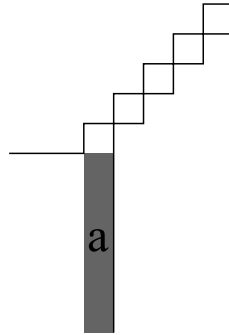


Figure 12: Configuration used to enlarge a Lagrangian grid diagram.

Proof. We may assume that G has an upper-right corner. Let $k \in \mathbb{Z}$. At the top right corner of the grid, we stabilize and attach a configuration of size $2k$ as shown in Figure 12. Since we began with a Lagrangian grid diagram, each new crossing created in this procedure will have $|\Delta t|$ equal to either $a \pm 1$ or a , and at the new top right corner, the t -coordinates will differ by $a \pm 1$. We then apply Lemma 3.13 to obtain a Lagrangian grid diagram. By carefully choosing which configurations we

use in applying Lemma 3.13, we may ensure that the Lagrangian grid diagram we obtain has even or odd size. The statement about the bound on Δ_2 is clear from the construction. \square

Corollary 8.3. *Given two Lagrangian grid diagrams, G and G' of size m and n , they may be stabilized to obtain Lagrangian grid diagrams representing the same two topological knots, without changing the rotation number, and such that if c_i is the set of crossings in G and c'_j is the set of crossings in G' , $|\Delta t(c_i)| < |\Delta t(c'_j)|$ for all i, j .*

Proof. Apply Theorem 8.1 to G , choosing k sufficiently large to guarantee that $k^2 > 4k + 1$ and $2k + 1 > \max\{\Delta t(c'_i)\} + |a| + 1$ where a is as shown in Figure 12. This guarantees that $\min\{\Delta t(c_i)\} > \max\{\Delta t(c'_i)\} + |a| + 1$. Then apply Theorem 8.2 to G' so that both grids are the same size. \square

Theorem 8.4. *Let G_{wy} and G_{zx} be Lagrangian grid diagrams of the same size such that if c_i is the set of crossings in G_{wy} and c'_j is the set of crossings in G_{zx} , then $|\Delta t(c_i)| \neq |\Delta t(c'_j)|$ for all i, j . Then, there is a Lagrangian hypercube diagram such that the wy and zx -projections are given by these grids.*

Proof. Following the orientation of the diagram label the markings $W_0, Y_0, W_1, Y_1, \dots$ etc. Do the same for G_{zx} . Denote the coordinates of W_i by $(w_{w,i}, y_{w,i})$, Y_i by $(w_{y,i}, y_{y,i})$ etc. Place Z_i in the hypercube at position $(w_{w,i}, x_{z,i}, y_{w,i}, z_{z,i})$, W_i at position $(w_{w,i}, x_{x,i}, y_{w,i}, z_{x,i})$, X_i at position $(w_{y,i}, x_{x,i}, y_{y,i}, z_{x,i})$, and Y_i at position $(w_{y,i}, x_{z,i+1}, y_{y,i}, z_{z,i+1})$ where i is taken modulo n . \square

Having developed the results on Lagrangian grid diagrams in Section 3, and having shown in Theorems 8.4, 8.2, and Corollary 8.3 we now have the necessary framework to complete the proof of Theorem 4 below.

Proof. Given $(m, k) \in \mathbb{Z}^2$, and two knot types K_1 and K_2 . Theorem 3.11 allows one to construct Lagrangian grid diagrams G_1 and G_2 representing K_1 and K_2 with rotation numbers m and k respectively. Corollary 8.3 allows one to find Lagrangian grid diagrams, G'_1 and G'_2 , of the same size representing the same topological knots and having the same rotation numbers as G_1 and G_2 . Applying Theorem 8.4 enables us to construct a Lagrangian hypercube diagram such that $G_{zx} = G'_1$ and $G_{wy} = G'_2$. \square

Example 8.5. One may construct a Lagrangian grid diagram for the unknot with arbitrary rotation number by following the construction shown in Figure 13. To realize rotation number $r > 0$ construct the diagram as in Figure 13 using $r + 1$ horizontal bars of length r . The resulting diagram will have size $2r + 3$. Let G_{zx} be such a grid diagram. Let G_{wy} be the Lagrangian grid diagram for the unknot of size $2r + 3$ given by the construction shown in Figure 14. Then applying Theorem 8.4, Lemma 6.1 and Theorem 1 we obtain a Lagrangian hypercube diagram with rotation class $(r, 0)$. Figure 10 shows the construction for $r = 1$.

Note that if $r = 0$ one must first apply Corollary 8.3. However, for $r > 1$, $|\Delta t(c_i)|$ is never equal to $|\Delta t(c)|$ where c is the unique crossing in G_{zx} and $\{c_i\}$ is the set of crossings in G_{wy} .

Example 8.6. Figure 15 shows a Lagrangian hypercube diagram with G_{zx} representing a trefoil, and G_{wy} representing a $(5, 2)$ torus knot. One may check that G_{wy} has rotation number 0, G_{zx} has rotation number 1, and hence, the Lagrangian hypercube diagram has rotation class $(1, 0)$.

REFERENCES

- [1] M. Aganagic, T. Ekhholm, L. Ng, C. Vafa. Topological Strings, D-Model, and Knot Contact Homology. arXiv:1304.5778 (2013).
- [2] S. Baldrige. Embedded and Lagrangian Tori in \mathbb{R}^4 and Hypercube Homology. arXiv:1010.3742.

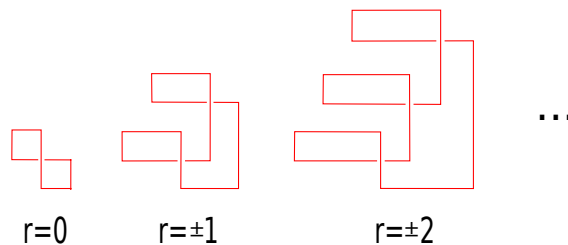


Figure 13: Construction of a Lagrangian unknots with rotation number $0, \pm 1, \pm 2$.

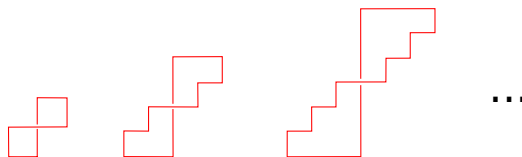


Figure 14: Construction of a Lagrangian unknots with rotation number 0 .

- [3] S. Baldridge, A. Lowrance. Cube diagrams and 3-dimensional Reidemeister-like Moves for Knots. *Journal of Knot Theory and its Ramifications*. DOI No: 10.1142/S0218216511009832.
- [4] S. Baldridge, B. McCarty. Small Examples of Cube Diagrams of Knots. *Topology Proceedings*. **36** (2010) pp. 213-228.
- [5] S. Baldridge, A. Lowrance. Cube Knot Calculator, <http://cubeknots.googlecode.com>.
- [6] I. Castro, F. Urbano. New examples of minimal Lagrangian tori in the complex projective plane. *Manuscripta Math.* **85** (1994) 265-281.
- [7] I. Castor, F. Urbano. On a minimal Lagrangian submanifold of \mathbb{C}^n foliated by spheres. *Michigan Mathematical Journal*. **46** (1999) 71-82.
- [8] P. Cromwell. Embedding knots and links in an open book. I. Basic properties. *Topology Appl.*, **64** (1995), no. 1, pp. 37-58.
- [9] T. Ekhholm, J. Etnyre, and M. Sullivan. Non-isotopic Legendrian submanifolds in \mathbb{R}^{2n+1} . *Journal of Differential Geometry*. Volume 71, Number 1 (2005), 85-128.
- [10] J. B. Etnyre, K. Honda. Knots and Contact Geometry I: Torus knots and the Figure Eight Knot. *Journal of Symplectic Geometry*. Volume 1, Number 1, (2001), pp. 63-120.
- [11] J. B. Etnyre. Legendrian and Transversal Knots. In the *Handbook of Knot Theory* (Elsevier B. V., Amsterdam), (2005), 105-185.
- [12] M. Haskins. Special Lagrangian cones. *American Journal of Mathematics*. Volume 126, No. 4, August 2004, 845-871.
- [13] D. Joyce. Special Lagrangian m -folds in \mathbb{C}^m with symmetries. *Duke Mathematical Journal*. Volume 115, No. 1 (1992).
- [14] C. Manolescu, P. Ozsvath, S. Sarkar. A combinatorial description of knot Floer homology. arXiv:math/0607691v2.
- [15] C. Manolescu, P. Ozsvath, Z. Szabo, D. Thurston. On combinatorial link Floer homology. arXiv:math/0610559v2.
- [16] B. McCarty. Cube number can detect chirality and Legendrian type of knots. *Journal of Knot Theory and its Ramifications*. DOI No: 10.1142/S0218216511009662.
- [17] B. McCarty. An infinite family of Legendrian torus knots distinguished by cube number. *Topology and its Applications*. DOI No: 10.1016/j.topol.2011.08.022.
- [18] D. McDuff, D. Salamon. *Introduction to Symplectic Topology*. Oxford University Press. 2nd Edition. (1999).
- [19] L. Ng. Computable Legendrian Invariants. *Topology*. Vol. 42, Issue 1, January 2003, pp. 55-82.
- [20] L. Ng. On arc index and maximal Thurston-Bennequin number. arXiv:math/0612356v3.
- [21] L. Ng, D. Thurston. Grid Diagrams, Braids, and Contact Geometry. *Proceedings of the 13th Goköva Geometric-Topology Conference*. pp. 1-17. (2008).
- [22] P. Ozvath, Z. Szabo, D. Thurston. Legendrian knots, transverse knots and combinatorial Floer homology. arXiv:math/0611841v2.
- [23] J. Robbin, D. Salamon. The Maslov Index for Paths. *Topology* **32** (1993), no. 4, 827 - 844.
- [24] A. Strominger, S.T. Yau, and E. Zaslow. Mirror symmetry and T-duality. *Nuclear Physics B*. **479** (1996) 243-259.

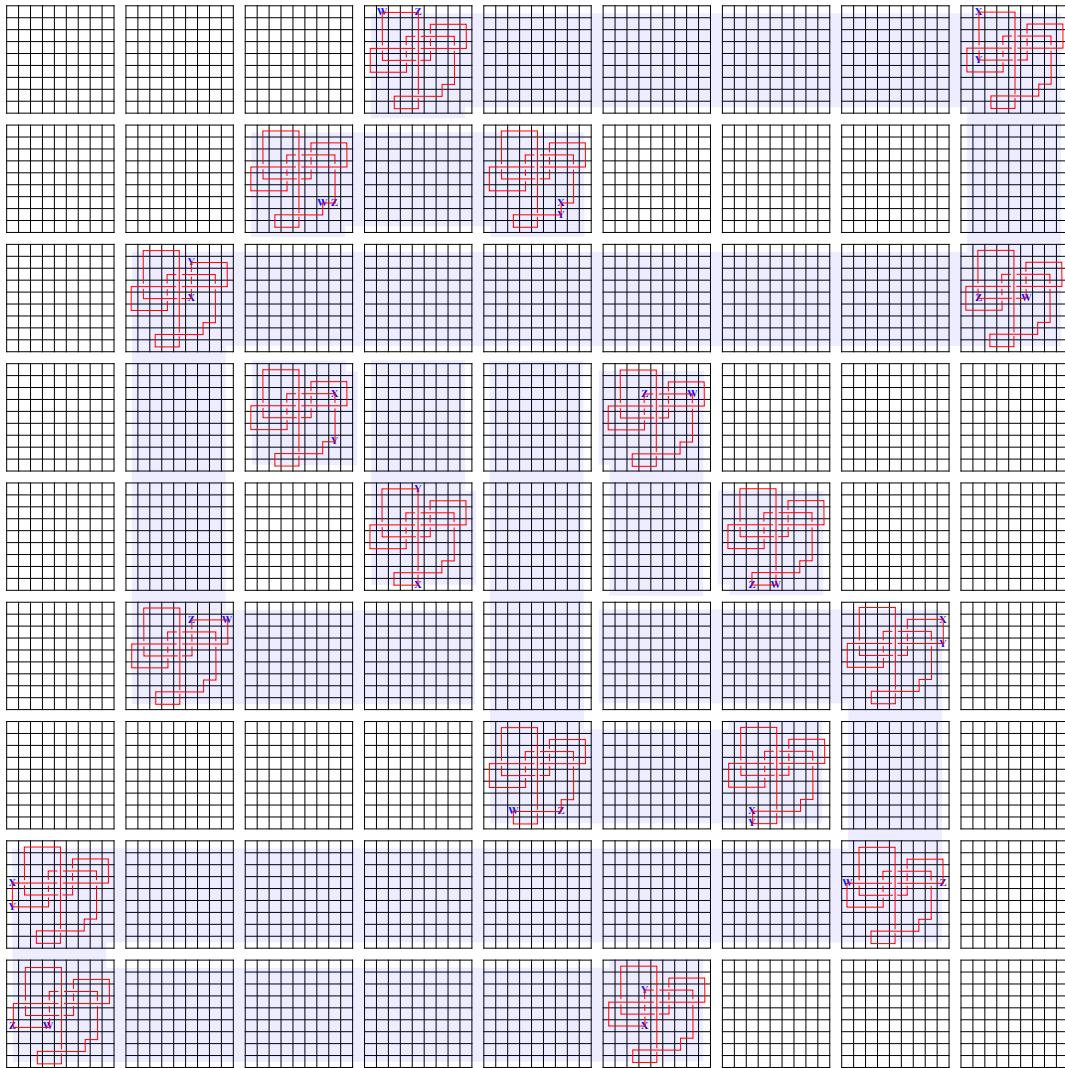


Figure 15: Hypercube diagram with G_{wy} representing a $(5,2)$ torus knot, and G_{zx} representing a trefoil.

- [25] S. Tabachnikov. An invariant of a submanifold that is transversal to a distribution, (Russian). *Uspekhi Mat. Nauk.* Volume 43, Number 3(261), (1988), 193194. Translation in *Russian Math. Surveys* 43 (1988), no. 3, 225226.
- [26] G. W. Whitehead. On mappings into group-like spaces. *Commentarii Mathematici Helvetici.* Volume 28, Number 1, 320-328, 1954.

DEPARTMENT OF MATHEMATICS, LOUISIANA STATE UNIVERSITY
 BATON ROUGE, LA 70817, USA
E-mail address: sbaldrid@math.lsu.edu

DEPARTMENT OF MATHEMATICAL SCIENCES, UNIVERSITY OF MEMPHIS
 MEMPHIS, TN, 38152, USA
E-mail address: bmmcrt1@memphis.edu